



INFLUENCE OF AGING TIME IN OBTAINING BIPHASIC CALCIUM PHOSPHATE (BCP) CERAMICS BY SOL-GEL METHOD

Lezli Matto¹, Lilian Paiva²,
Alexandre Antunes Ribeiro²,
Magna M Monteiro¹

¹Bio and Materials Laboratory, Polytechnic Faculty, National University of Asuncion. San Lorenzo, Central, Paraguay.

²Powder Technology Laboratory, Materials Processing and Characterization Division, National Institute of Technology, Rio de Janeiro, RJ, Brazil.

E-mail: lezligiselle@gmail.com

ABSTRACT

Calcium phosphate ceramics have shown a wide range of applicability in orthopedic and dental areas, substituting or repairing lost or damaged body parts. Specifically, biphasic calcium phosphates (BCP) get a special attention due to their controlled bioactivity and equilibrium, between resorption/solubilization processes, when in contact with body fluids. The present work aimed to study the influence of aging time in obtaining of BCP by sol-gel method, composed of hydroxyapatite and β -tricalcium phosphate phases. The samples were aged in oven for 24, 48, 72 and 96 hours at 60°C and characterized by Fourier Transform Infrared Spectroscopy and X-ray Diffraction techniques. According to the results, the aging time played a fundamental role on the calcium phosphates phases and on the crystallinity of samples. Under such conditions, the optimal routes for obtaining BCP were those corresponding to the aging times of 24 and 72 hours. However, the sample aged for 72 hours presented greater crystallinity in comparison with the sample aged for 24 hours, evincing the influence of aging time on BCP.

Keywords: Biphasic calcium phosphate ceramics; sol-gel synthesis; aging time; crystallinity; biomaterials.

1. INTRODUCTION

In biomaterials field, calcium phosphates are known for their biocompatibility and optimal biological response from host tissue, due to similarity to the mineral phase of bone. They have a wide range of applicability in orthopedic and dental field, substituting or repairing damaged or lost body parts.

Hydroxyapatite (HAp), tricalcium phosphate (TCP), and their biphasic combinations (BCP) constitute important bioceramic materials for replacement of hard tissues, as a result of a strong bond with mineral content, inducing bone formation (Vallet-Regí and González-Calbet, 2004).

Certain phases of these compounds are more stable than others when in contact with body fluids. Therefore, their applications depend on specific characteristics. Chemical

composition of a bioceramic influences in the rate of solubilization/resorption as well as on its bioactivity. For instance, while HAp is slowly resorbed and/or solubilized, β -TCP undergoes a much faster process of resorption (Lobo and Arinzeh, 2010).

Several synthetic routes have been developed to prepare BCP bioceramics of variable HA/ β -TCP ratios, simulating the physical and biological properties of natural bones. Nevertheless, up to now, there has been relative success in the fabrication of bone substitute materials similar to natural bone (Ebrahimi *et al.*, 2017).

Synthetic bioceramics may exhibit chemical and processing defects that modify their morphology, crystallinity, surface properties and reactivity in the body, restraining the application as a biomaterial. Protocols have been proposed, and variables such as total time of synthesis were investigated, to study their effect on the final HAp product, to achieve the optimal single or biphasic calcium phosphate end product for a predesigned function (Ben-Arfa *et al.*, 2017).

Sol-gel method gives excellent control of product purity and composition since it starts from pure materials (Carter and Norton, 2007). Using this method for the preparation of HAp makes possible the obtention of fine-grain microstructure containing nano to submicron particles with crystalline structure (Bakan *et al.*, 2013). It enables a molecular-level mixing of the calcium and phosphorus precursors, which can improve chemical homogeneity of the resulting HAp to a significant extent in comparison with conventional methods (Liu *et al.*, 2001).

Nevertheless, the ideal physicochemical properties of BCP for bone applications have not been defined up to the present time. The reason is mostly related to the lack of standard study protocols in biomaterial science, especially with regards to their characterizations and clinical applications (Ebrahimi *et al.*, 2017).

This work aims to validate a production route of calcium phosphates bioceramics developed in the Bio and Materials Laboratory of the Polytechnic School of the National University of Asunción. The synthesized samples were characterized by Fourier Transform Infrared (FTIR) and X-ray diffraction (XRD), in order to determine the functional groups, and crystallinity, and to identify and quantify the present phases semi-quantitatively.

2. MATERIALS AND METHODS

For the synthesis of BCP, an alcoholic solution of calcium nitrate tetra-hydrated ($\text{Ca}(\text{NO}_3)_2 \cdot 4\text{H}_2\text{O}$) of 1.67 M and an aqueous solution of ammonium acid phosphate ($(\text{NH}_4)\text{HPO}_4$) of 1M were prepared. The reagents used were PA, all from Cicarelli®, Argentina. The calcium precursor was prepared by weighing 19.706 g of calcium nitrate tetrahydrated, which was dissolved in 50 mL of ethanol. For the phosphorus precursor solution, 6.60 g of ammonium acid phosphate was weighed, which was dissolved in 50 mL of distilled water. The solutions were mixed with a peristaltic pump (LongerPump model BT100-2J). After the complete addition, the mixture remained under constant stirring at 40°C for 30 min. A flux chart of the process is presented in Fig. 1.

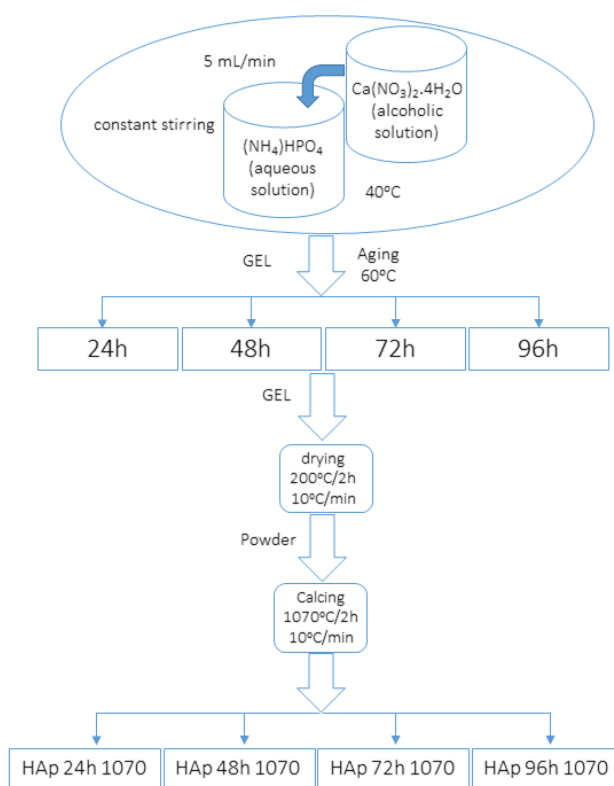


Figure 1. Flux chart of the procedure for synthesis of calcium phosphate.

After synthesis, the obtained white gel was aged at 60°C for 24, 48, 72 and 96 hours in oven (QUIMIS, Brazil). After aging, the gel was dried in a muffle (Nobertherm, Germany) at 200°C/2h with 10°C/min heating rate. Finally, the powders were heat treated (calcined) at 1070°C/2h, also with 10°C/min heating rate. The calcination temperature was chosen in order to achieve partial transformation of HAp into β -TCP and to obtain good crystallinity.

For infrared analysis (FTIR), the iD1 accessory was used, with which it was possible to analyze the samples by transmission, reaching a greater range. Samples were analyzed in the range of 4000-400 cm^{-1} , with 4 cm^{-1} resolution and 128 scans. KBr pellets were used, with 2 mg of sample dispersed in 100 mg of KBr and compacted at 80 kN for 3 min. This technique was used to identify the absorption bands of functional groups.

In the X-ray diffraction analysis (XRD), the samples were analyzed in the range of $10^\circ \leq 2\theta \leq 60^\circ$, with copper anode (Cu, $\lambda = 0.15405\text{nm}$), $K\alpha$ radiation generated at 45kV and 40 mA with 0.01° step size and 5 s/step. This technique was used to verify the crystalline phases, determine the crystallinity and the relation of phases.

Maximum intensity peak values of each phase were used to determine the relative fractions of the phases. This was calculated by the RIR equation (Relative Intensity Ratio) as it is shown below:

$$\text{RIR}_{\beta\text{-TCP}} = \frac{I_{\beta\text{-TCP}}}{(I_{\text{HAp}} + I_{\beta\text{-TCP}})}$$

Ec. 1.

Where, I_{HAp} and $I_{\beta\text{-TCP}}$ are the intensities for hydroxyapatite and β -tricalcium phosphate phases at their position of maximum intensity, respectively. According to the ICDD (International Center for Diffraction Data) the position of the maximum intensity for HAp is $2\theta = 31.8^\circ$ and for β -TCP it is $2\theta = 31^\circ$.

3. RESULTS

In table 1, a list of characteristic absorption bands of calcium phosphates, as found in literature, is presented.

Table 1. Absorption bands characteristics of the calcium phosphates.

Group	Band (cm^{-1})	Reference	Observation
OH ⁻	630	Stoch <i>et al.</i> , 1999, Raynaud <i>et al.</i> , 2002, Destainville <i>et al.</i> , 2003 and Vani <i>et al.</i> , 2009.	Corresponding to crystalline HAp.
	3570	Stoch <i>et al.</i> 1999. Han J-K. <i>et al.</i> , 2006.	O-H vibrational mode corresponding to crystalline HAp.
adsorbed water (H ₂ O)	3440	Kwon <i>et al.</i> , 2003 and Vani <i>et al.</i> , 2009.	H-O-H deformation due to presence of water.
	1660	Raynaud <i>et al.</i> , 2002, Han J-K. <i>et al.</i> , 2006 and Bakan <i>et al.</i> , 2013.	Bending mode of hydroxyl group in adsorbed water.
PO	1030	Han J-K. <i>et al.</i> , 2006 and Vani <i>et al.</i> , 2009.	ν_3 , P-O asymmetric stretching mode.
	563	Han J-K. <i>et al.</i> , 2006.	Stretching mode.
PO ₄ ³⁻	460	Raynaud <i>et al.</i> , 2002 and Destainville <i>et al.</i> , 2003.	ν_2 , O-P-O bending mode.
	550 – 610	Stoch <i>et al.</i> , 1999, Raynaud <i>et al.</i> , 2002, Destainville <i>et al.</i> , 2003, Kwon <i>et al.</i> , 2003 and Mobasherpour and Heshajin, 2007.	ν_4 , O-P-O bending mode.
	1000 – 1120	Raynaud <i>et al.</i> , 2002, Destainville <i>et al.</i> , 2003 and Mobasherpour and Heshajin, 2007.	ν_3 asymmetric stretching.
	1040	Han J-K. <i>et al.</i> , 2006.	Bending mode.
HPO ₄ ²⁻	970	Fazardi <i>et al.</i> , 2011.	HPO ₄ ²⁻ in β -TCP.
P ₂ O ₇ ⁴⁻	725 and 1200	Destainville <i>et al.</i> , 2003.	Corresponding to Ca ₂ P ₂ O ₇ .
	723, 1185 and 1210	Boilet <i>et al.</i> , 2013.	



Figure 2 displays the spectra of samples synthesized in the present work. The spectrum of HAp24h1070 sample shows the characteristic band of hydroxyl group (3570 and 637 cm^{-1}), bands of adsorbed water around at 3422 and 1657 cm^{-1} and PO_4^{3-} bands (1092, 1046, 971, 604 and 570 cm^{-1}) related to HAp phase. In this spectrum, the band assigned to HPO_4^{2-} functional group (970 cm^{-1}) can be clearly identified, which corresponds the presence of β -TCP phase (Fazardi *et al.*, 2011).

In HAp48h1070 spectrum, it is possible to observe the following bands related to HAp phase. The bands corresponding to adsorbed water (3422 and 1657 cm^{-1}) have decreased considerably. The hydroxyl bands are still present (3570 cm^{-1} and 631 cm^{-1}) and also those of PO_4^{3-} group (1093, 1047, 973, 605 and 570 cm^{-1}). A band appears near 460 cm^{-1} , which is related to bending mode, ν_2 , of PO_4^{3-} (Raynaud *et al.*, 2002; Destainville *et al.*, 2003). In this sample, the bands around 1200 cm^{-1} , 725 cm^{-1} and 1185 cm^{-1} are characteristic of the vibrational modes of $\text{P}_2\text{O}_7^{4-}$ (Boilet *et al.*, 2013; Destainville *et al.*, 2003) attributed to calcium pyrophosphate (CPP - $\text{Ca}_2\text{P}_2\text{O}_7$), which is an undesirable phase for biomedical applications. CPP is known to induce the occurrence of certain diseases, caused by intra or extra-articular deposits of pyrophosphate crystals (Ottaviani *et al.*, 2013), although some authors report it is possible to administer pyrophosphate systemically in order to prevent or reduce uremia-related vascular calcification, without causing negative consequences for bone or diseases related to pyrophosphate deposit (Persy and McKee, 2011).

For HAp72h1070 sample, crystalline HAp hydroxyl bands are clearly seen at 3575 and 640 cm^{-1} , which appear more intense than in other samples, assuming a greater crystallinity. Also, the bands of PO_4^{3-} group (1093, 1047, 964, 605, 570 and 473 cm^{-1}) can be identified. Due to the absence of characteristic bands of CPP and comparing these results with those obtained by XRD, it is possible to confirm that this sample is constituted by a crystalline biphasic calcium phosphate (BCP) only.

In the spectra of HAp96h1070 sample, the PO_4^{3-} (1088, 1043, 972, 607, 550 and 457 cm^{-1}) and adsorbed water (3430 and 1640 cm^{-1}) bands are found, and they are related to HAp phase. Here, the characteristic vibrational modes of the hydroxyl are no longer present, which could be due to perturbations of stretching and bending modes of superficial hydroxyl group in apatite by the hydrogen bonds with water molecules (Stoch *et al.*, 1999). This sample shows large peaks near 1210, 1185 and 725 cm^{-1} ascribed to the vibrational modes of pyrophosphate (CPP), indicating that under such conditions the CPP phase is formed again.

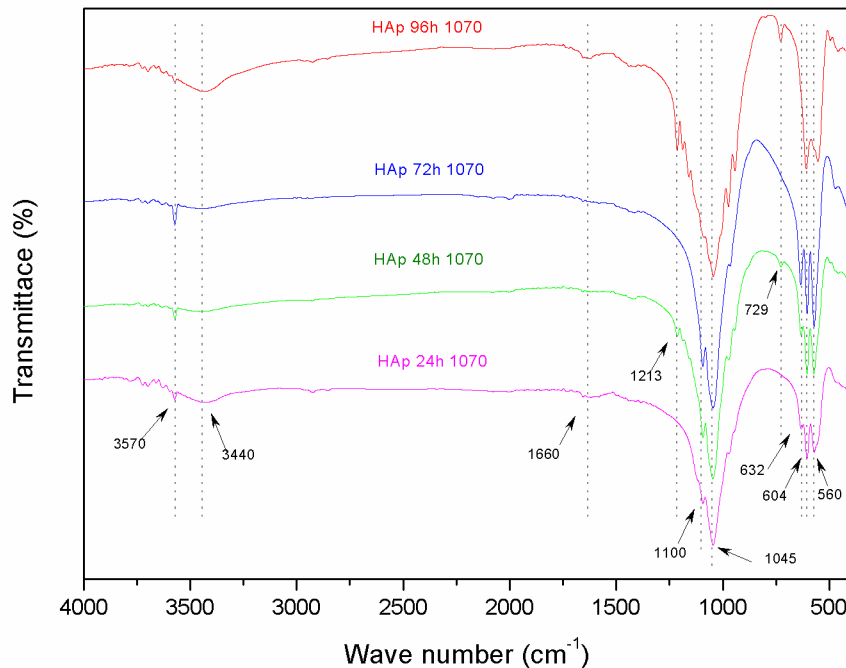


Figure 2. FTIR spectra of the calcium phosphate samples synthesized under different conditions.

Figure 3 shows the X-ray diffractograms of the samples, comparing the positions and intensities of the characteristic peaks for each phase. According to XRD results, the presence of HAp (ICDD N° 00-009-0432) and β -TCP (ICDD N° 00-009-0169) were identified in all samples. However, it was not possible to identify the CPP (ICDD N° 01-071-2123) characteristic peaks, due to the overlaps of peaks related to CPP and β -TCP, particularly the peaks of greater intensities. According with FTIR results and from Figs. 2 and 3, it is noted that HAp24h1070 and HAp72h1070 samples are formed by a biphasic calcium phosphate (BCP) composed of HAp and β -TCP phases. The relative amount of each phase was calculated by Eq. 1 and the values are exhibited in Table 2. From these values, it can be verified that the relative amount of β -TCP in HAp72h1070 sample is approximately 10% higher than HAp24h1070 sample, which was expected, since the aging time is longer and therefore favors formation or transformation of the crystalline phases.

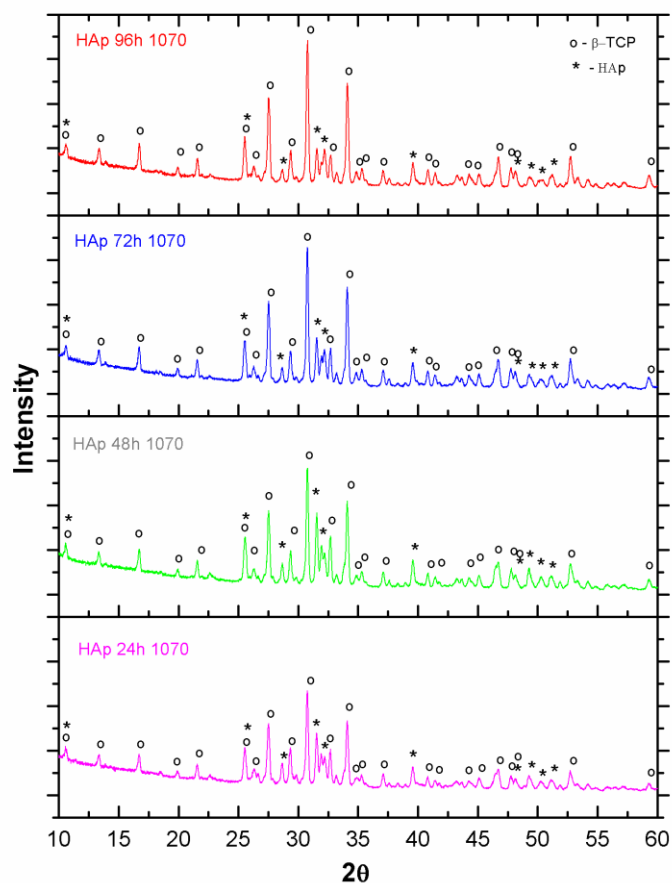


Figure 3. XRD Patterns of the calcium phosphates synthesized under different conditions.

Table 2. Quantification of the HAp and β -TCP phases, for HAp72h1070 and HAp24h1070 samples.

HAp72h1070			
Crystalline phase	Bragg angle (2θ)	I_{\max}	%
Hap	31.774	2515	27,6%
β -TCP	31.027	6613	72,4%
HAp24h1070			
Crystalline phase	Bragg angle (2θ)	I_{\max}	%
Hap	31.774	2790	37,3%
β -TCP	31.027	4688	62,7%

Figure 4 compares the diffractograms of HAp24h1070 and HAp72h1070 samples, in order to visualize the difference of the peak heights. Comparing the maximum intensity peaks, it is suggested that HAp72h1070 sample has the highest crystallinity, since its maximum intensity peaks are greater than those for HAp24h1070 sample. This analysis could not be done for HAp48h1070 and HAp96h1070 diffractograms, because CPP and β -TCP peaks are very close to each other, causing a constructive interference in 2θ around 29.6° . Further, XRD results agree with FTIR data, because in the FTIR spectrum of HAp72h1070 sample (Fig. 2) it was verified that the band assigned to crystalline hydroxyapatite appears more pronounced than in spectra for other samples.

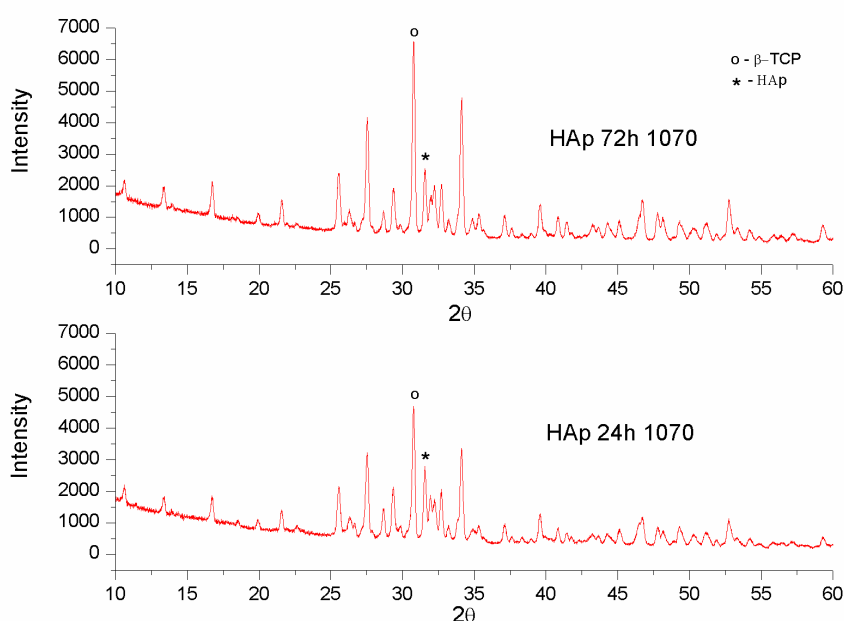


Figure 4. Comparison of Hap72h1070 and Hap24h1070 diffractograms.

4. CONCLUSION

Based on the results, it is concluded that aging time (AT) plays a fundamental role in the synthesis of calcium phosphates (CaP) bioceramics, since AT variation induced the formation of different CaP phases with different concentrations. Moreover, AT affected the crystallinity of the samples, where the highest crystallinity was observed for HAp72h1070 sample.

Considering CaP phase compositions and crystallinity level, the optimal routes for obtaining biphasic calcium phosphate (BCP) were those of HAp24h1070 and HAp72h1070 samples. However, HAp72h1070 sample presented desirable composition, since CPP phase was not detected among HAp and β -TCP phases. Then, the time of 72 hours can be considered an ideal AT for BCP synthesis by sol-gel method.



REFERENCES

- Bakan, F.; Laçin, O. and Sarac, H. (2013). A novel low temperature sol–gel synthesis process for thermally stable nanocrystalline hydroxyapatite. *Powder Technol*, 233, 295-302.
- Ben-Arfa, B. A. E.; Miranda Salvado, I. M.; Ferreira, J. M.F. and Pullar, R. C. (2017). Novel route for rapid sol-gel synthesis of hydroxyapatite, avoiding ageing and using fast drying with a 50 - fold to 200 - fold reduction in process time. *Materials Science and Engineering. C* 70, 796 - 804.
- Boilet, L.; Descamps, M.; Rguiti, E.; Tricoteaux, A.; Lu, J.; Petit, F. and Leriche, A. (2013). Processing and properties of transparent hydroxyapatite and β tricalcium phosphate obtained by HIP process. *Ceram Int.*, 39, 283-288.
- Carter, C.B. and Norton, M.G., (2007). *Ceramic Materials: Science and Engineering*. Springer New York.
- Destainville, A.; Champion, E.; Bernache-Assollant, D. and Laborde, E. (2003). Synthesis, characterization and thermal behavior of apatitic tricalcium phosphate. *Materials Chemistry and Physics*, 80, 269-277.
- Dorozhkin, S. V., (2010). Bioceramics of calcium orthophosphates. *Biomaterials*, 31, 1465-1485.
- Ebrahimi, M.; Botelho, M. G. and Dorozhkin, S.V. (2017). Biphasic calcium phosphates bioceramics (HA/TCP): Concept, physicochemical properties and the impact of standardization of study protocols in biomaterials research. *Materials Science and Engineering. C* 71, 1293-1312.
- Fathi, M. F.; Hanifia, A. and Mortazavi, V. (2008). Preparation and bioactivity evaluation of bone-like hydroxyapatite nanopowder. *Journal of materials processing technology*, 202, 536-542.
- Farzadi, A.; Solati-Hashjin M.; Bakhshi, F. and Aminian, A. (2011). Synthesis and characterization of hydroxyapatite/b-tricalciumphosphate nanocomposites using microwave irradiation *Ceramics International* 37, 65-71.
- Han J. K.; Song, H. Y.; Saito, F. and Lee, B. T. (2006). Synthesis of high purity nano-sized hydroxyapatite powder by microwave-hydrothermal method. *Materials Chemistry and Physics*, 99, 235 - 239.
- Know, S-H; Jun, Y-K; Hong, S-H and Kim, H-E. (2003). Synthesis and dissolution behavior of b-TCP and HA/b-TCP composite powders. *Journal of the European Ceramic Society*, 23, 1039-1045.
- Liu, D. M.; Troczynski, T. and Tseng, W. J. (2001). Water-based sol-gel synthesis of hydroxyapatite: process development. *Biomaterials*, 22, 1721-1730.
- Lobo, S. E. and Arinzeh, T. L. (2010). Biphasic Calcium Phosphate Ceramics for Bone Regeneration and Tissue Engineering Applications. *Materials*, 3, 815-826.



- Mobasherpour, I.; Soulati Heshajin, M.; Kazemzadeha, A. and Zakeri, M. (2007). Synthesis of nanocrystalline hydroxyapatite by using precipitation method. *Journal of Alloys and Compounds* 430, 330 - 333.
- Ottaviani, S.; Brunier, L.; Sibilia, J.; Maurier, F.; Ardizzone, M.; Wendling, D.; Gill, G.; Palazzo, E.; Meyer, O. and Dieudé, P. (2013) Efficacy of anakinra in calcium pyrophosphate crystal induced arthritis: a report of 16 cases and review of the literature. *Joint Bone Spine*. 80, 178-182.
- Persy, V. P. and McKee, M. D. (2011). Prevention of vascular calcification: is pyrophosphate therapy a solution? *Kidney International*. 79, 5, 490 – 493.
- Ramakrishna, S.; Ramalingam, M.; Kumar, T.S.S. and Soboyejo, W.O. (2010) *Biomaterials: A Nano Approach*. CRC Press.
- Raynaud, S.; Champion, E.; Bernache-Assollant D. and Thomas, P. (2002). Calcium phosphate apatites with variable Ca/P atomic ratio I. Synthesis, characterization and thermal stability of powders. *Biomaterials*, 23, 1065-1072.
- Stoch, A.; Jastrzębski, W.; Broek, A.; Trybalska, B.; Cichociska, M. and Szarawara, E. (1999). FTIR monitoring of the growth of the carbonate containing apatite layers from simulated and natural body fluids. *Journal of Molecular Structure*, 511-512, 287-294.
- Vallet-Regí, M. and González-Calbet, J. M. (2004). Calcium phosphates as substitution of bone tissues. *Progress in Solid State Chemistry*, 32, 1-31.
- Vani, R.; Girija, E. K.; Elayaraja, K.; Prakash Parthiban, S.; Kesavamoorthy, R. and NarayanaKalkura, S., (2009). Hydrothermal synthesis of porous triphasic hydroxyapatite/ (a and b) tricalcium phosphate. *Journal of Materials Science: Materials in Medicine*, 20, 43-48.